ACS APPLIED MATERIALS & INTERFACES

RESEARCH ARTICLE

www.acsami.org

Tough Graphene−Polymer Microcellular Foams for Electromagnetic Interference Shielding

Hao-Bin Zhang,[†,‡] Qing Yan,[‡] Wen-Ge Zheng,[*,‡] Zhixian He,[†] and Zhong-Zhen Yu[*,†]

[†]Beijing Key Laboratory on Preparation and Processing of Novel Polymeric Materials, Department of Polymer Engineering, College of Materials Science and Engineering, Beijing University of Chemical Technology, Beijing 100029, China

[‡]Ningbo Key Laboratory of Polymer Materials, Division of Polymers and Composites, Ningbo Institute of Materials Technology & Engineering, Chinese Academy of Sciences, Ningbo 315201, China

Supporting Information

ABSTRACT: Functional polymethylmethacrylate (PMMA)/graphene nanocomposite microcellular foams were prepared by blending of PMMA with graphene sheets followed by foaming with subcritical CO_2 as an environmentally benign foaming agent. The addition of graphene sheets endows the insulating PMMA foams with high electrical conductivity and improved electromagnetic interference (EMI) shielding efficiency with microwave absorption as the dominant EMI shielding mechanism. Interestingly, because of the presence of the numerous microcellular cells, the graphene−PMMA foam exhibits greatly improved ductility and tensile toughness compared to its bulk counterpart. This work provides a promising methodology to fabricate tough and lightweight graphene−PMMA nanocomposite microcellular foams with superior electrical and EMI shielding properties by simultaneously combining the functionality and reinforcement of the graphene sheets and the toughening effect of the microcellular cells.

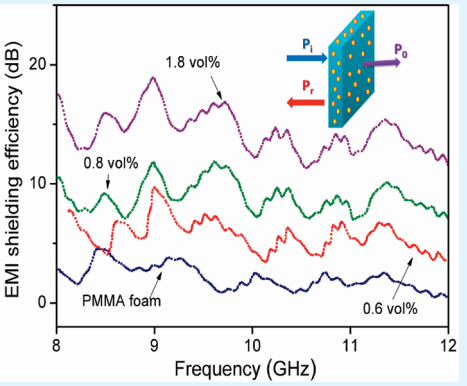

KEYWORDS: graphene, microcellular foam, electrical conductivity, electromagnetic interference shielding, polymethylmethacrylate

INTRODUCTION

Graphene has recently gained revolutionary aspirations because of its remarkable electronic, thermal, and mechanical properties. These unique properties make it promising to prepare multifunctional composites.[1−7] With the extensive practical applications of sensitive electronic devices and densely packed systems, electromagnetic interference (EMI) becomes a more and more serious problem. Thus, much attention has been paid to the development of novel EMI shielding materials.[8−13] Compared to the conventional metal-based EMI materials, electrically conductive polymer composites have their own advantages, such as light weight, resistance to corrosion, good processability, and tunable conductivity. The electrical conductivity and EMI shielding efficiency of these polymer composites depend mainly on intrinsic conductivity, aspect ratio, and content of the fillers.[10,14,15] The high aspect ratio and electrical conductivity of graphene sheets and carbon nanotubes (CNTs) facilitate the improvement of electrical and EMI shielding properties without significantly sacrificing other properties of the matrix polymers.[4,5,12,15,16]

Light weight is very important and favorable for the practical EMI shielding application in the areas of aircraft, spacecraft, and automobiles, because it would save materials and energy. To further reduce the density of these polymer composites, researchers preferred foam structures which could be easily formed by using many techniques.[13,17−19] The resulting polymer composite foams might still exhibit high electrical conductivity and high EMI shielding efficiency, although the conductive network in the matrix would inevitably be impaired. Gupta et al.[18,19] reported an EMI shielding effectiveness (SE)of ∼20 dB for polystyrene nanocomposite foam with 7 wt % CNTs in the frequency range of 8.2−12.4 GHz, much higher than that (∼9 dB) of the polystyrene foams with 7 wt % carbon nanofibers. Li et al.[17] prepared ultralight polyurethane/CNT foams with superior electrical conductivity. Recently, Jerome et al.[13] reported an EMI SE as high as 60−80 dB in polycaprolactone/CNT foams with a main shielding mechanism of absorption rather than reflectivity. Although CNTs have received much attention as they impart insulating polymers with high electrical and EMI shielding properties, their wider applications are still limited because of their disadvantages, such as high cost, impurities from the catalysts, bundling, and aggregation.[20] By contrast, graphene sheets are believed to be an alternative of CNTs to prepare multifunctional polymer nanocomposites and foams, because of their high specific surface area, high aspect ratio, and layered structure.[21]

In addition, tensile strength, ductility, and fracture toughness are also important properties for the application of polymer foams. It is noted that if the pores in polymer foam are very large, they would readily evolve to large cracks and make the foam brittle. Interestingly, microcellular foams can provide increased toughness, improved fatigue life and energy absorption.[22,23] To the best of our knowledge, few papers have been focused on electrically conductive graphene−polymer microcellular foams.[24] Therefore, the purpose of

Received: January 7, 2011
Accepted: February 15, 2011
Published: March 02, 2011

Table 1. Density Values of Graphene−PMMA Bulk and Foams with Different Graphene Contents

graphene content in bulk (wt%)	graphene content in bulk (vol%)	density of bulk (g cm^{-3})	graphene content in foam (vol%)	density of foam (g cm^{-3})
0.5	0.3	1.19	0.2	0.65
1.0	0.5	1.20	0.3	0.58
1.2	0.6	1.20	0.4	0.67
2.0	1.1	1.20	0.6	0.65
3.0	1.6	1.21	0.8	0.61
5.0	2.7	1.22	1.8	0.79

the present study is to fabricate electrically conductive polymethylmethacrylate (PMMA) nanocomposite by using graphene sheets as the conducting filler and then to make the brittle nanocomposite ductile by foaming with the aid of subcritical CO_2 foaming technique. The graphene−PMMA nanocomposite microcellular foams were investigated in terms of microstructure, electrical conductivity, EMI shielding efficiency, and mechanical properties. Because graphene sheets are efficient in improving both electrical and mechanical properties of polymers,[4,25,26] it is expected that the graphene−PMMA nanocomposite foams would exhibit superior EMI shielding efficiency and improved electrical and mechanical properties.

EXPERIMENTAL SECTION

2.1. Materials. Graphene sheets were prepared according to the method described in our previous work[27,28] (see the Supporting Information). The specific surface area of the graphene is ~700 m^2/g, measured with a Micromeritics ASAP 2010 analyzer (Norcross, GA) in terms of Brunauer, Emmett and Teller (BET) method using nitrogen adsorption. TEM observation indicates that each platelet is composed of ~3−4 individual graphene sheets.[28] General grade PMMA pellets with a trade name of CM207 were purchased from Zhenjiang Chimei Corporation (China). Its density and weight-average molecular weight are 1.19 g/cm^3 and 96,800 g/mol, respectively. Methylene dichloride was supplied by Sinopharm Chemical Reagent (China) and used as received.

2.2. Fabrication of Graphene−PMMA Nanocomposites. The graphene−PMMA nanocomposites were prepared by solution blending and melt compounding. For solution blending, stable suspension of graphene sheets in methylene dichloride was first prepared by ultrosonication, and then mixed with PMMA. After being stirred for 4 h, the homogeneous suspension was poured onto glass plates and heated to remove the solvent. The samples used for conductivity measurements and foaming were prepared by hot-pressing at 190 °C. For melt compounding, PMMA and graphene sheets were melt-compounded on a Brabender Mixer at 190 °C with an initial speed of 50 rpm for 2 min followed by 100 rpm for 3 min; the resulting nanocomposites were then injection-molded into dumbbell bars for tensile tests. The weight and volume content of graphene sheets in bulk PMMA nanocomposites as well as their density were listed in Table 1.

2.3. Preparation of PMMA Nanocomposite Microcellular Foams. All PMMA foams were prepared by a batch foaming process with the aid of subcritical CO_2. The bulk samples were saturated with CO_2 at given conditions (0−25 °C, 3.5−5.0 MPa and 24 h) in a pressure vessel. The saturation condition used here depends on the thickness of bulk samples. For samples thinner than 2 mm, the conditions were 25 °C, 5.0 MPa and 24 h; while for tensile specimens with a thickness of 4 mm, the conditions of 0 °C, 3.5 MPa, and 24 h were used to achieve adequate saturation.[23] After the complete saturation, the pressure was rapidly released and the samples were quickly immerged in a preheated hot water for certain time. Then, the morphology of the foam was fixed in an ice/water mixture. Table 1 lists the density values of PMMA nanocomposite foams with different graphene contents, which were prepared at the same saturation (25 °C, 5.0 MPa, and 24 h) and foaming (70 °C) conditions.

2.4. Characterizations. The microstructures of the foams were observed with a Hitachi S-4800 scanning electron microscopy (SEM). The samples were freeze-fractured after immersion in liquid nitrogen for 20 min and the fractured surfaces were coated with a thin layer of platinum before the SEM observation. The dispersion and distribution of the graphene sheets were examined with a Tecnai G2 F20 transmission electron microscopy (TEM) at an accelerating voltage of 100 kV. The samples were embedded in epoxy resin and cured at 80 °C for 6 h, and then ultrathin sections thinner than 100 nm were cryogenically cut with a diamond knife using a microtome and collected on 300-mesh copper grids. The volume conductivity of the moderately conductive samples (>1 × 10^{-6} S/m) was measured using a standard four-probe method on a Physical Property Measurement System (Quantum Design, US). The samples with low conductivities (≤1 × 10^{-6} S/m) were measured with a three-terminal fixture on an EST121 ultrahigh resistance and micro current meter (Beijing EST Science & Technology CO. Ltd.) according to ASTM D257. Circular plates with 7 cm in diameter were fabricated for conductivity measurements. The sample surfaces were coated with silver paste to reduce contact resistance between the sample and the electrodes. The EMI SE of the samples was measured at room temperature in the frequency range of 8−12 GHz using a WILTRON 54169A scalar measurement system. The microcellular foams were cut to rectangle plates with a dimension of 22.9 × 10.2 mm^2 to fit the waveguide sample holder. All the foam samples are ~4 mm in thickness except for the PMMA foam with 1.8 vol % graphene sheets (2.4 mm thick). The tensile properties were measured on an Instron 5567 testing machine at a crosshead speed of 2.8 mm/min. At least five specimens were tested for each composition and mean values were reported.

RESULTS AND DISCUSSION

Figure 1a shows a representative SEM micrograph of the cross-section of the graphene−PMMA nanocomposite foam with 1.8 vol % graphene sheets. It is evident that the microcellular cells with an average size of ~5 μm were distributed throughout the foam. These nearly spherical cells exhibit a cell size distribution from 1 to 10 μm. This microcellular structure may offer advantages in improving electrical and mechanical properties of the foam over the polymer foams with larger cells that filled with carbon nanofibers and nanotubes.[13,18,19] The formation of this unique microcellular structure is attributed to the use of subcritical CO_2 as the foaming agent. After the completely saturated graphene−PMMA nanocomposites were rapidly taken out from the pressure vessel and quickly immerged in hot water, the CO_2 became supersaturated in the nanocomposites and was released, resulting in the formation of numerous cells. The well-defined cell size and structure homogeneity could be readily gained by adjusting the saturation and foaming conditions during the foaming process. It is worth noting that even a low loading of graphene sheets were efficient in inducing the heterogeneous nucleation of cells and decreasing the cell sizes of the PMMA foam (see Figure S1 in the Supporting Information).

Just like other polymer foams filled with inorganic fillers,[13,17−19] the graphene−PMMA foam is a ternary system composed of PMMA matrix, graphene sheets and pores. The distribution of graphene sheets plays an important role in determining the electrical conductivity and EMI shielding efficiency of the PMMA foam. Figure 1b shows a TEM micrograph of the well-dispersed graphene sheets in a cell wall of the PMMA nanocomposite foam with 0.8 vol % graphene sheets. It is clear that the graphene sheets were homogeneously dispersed and located in the cell wall, forming an interconnected graphene network throughout the cell walls and struts of

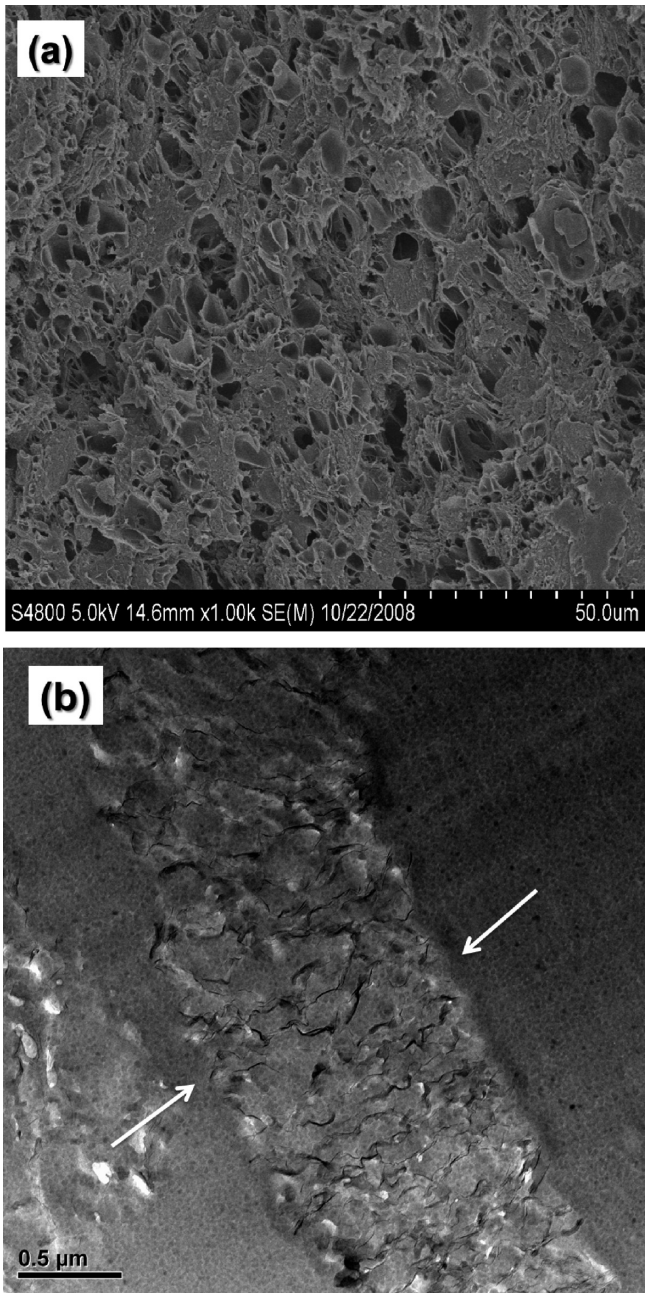

Figure 1. (a) SEM image of the cross-section of PMMA nanocomposite microcellular foam with 1.8 vol % graphene sheets; (b) TEM image of well-dispersed graphene sheets in a cell wall of the PMMA nanocomposite microcellular foam with 0.8 vol % graphene sheets. The arrows point to the cell wall surfaces.

the foam. This continuous conducting network is responsible for the improved electrical conductivity and EMI shielding efficiency.[15,17]

Electrical conductivity is of utmost importance for EMI shielding efficiency, because it is an intrinsic ability of a material to absorb electromagnetic radiation. The inclusion of pores in the graphene−PMMA nanocomposite greatly decreased the density of the nanocomposite as well as the actual volume content of graphene sheets. Figure 2 shows the electrical conductivity versus graphene content for the graphene−PMMA bulk nanocomposites and foams. It is seen that the electrical conductivity increases with the increase of graphene content for both the bulk and foamed nanocomposites.

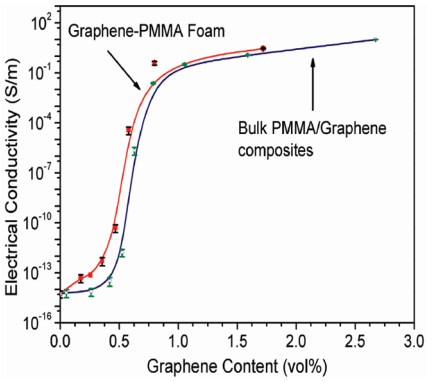

Figure 2. Plots of electrical conductivity versus graphene content for graphene−PMMA bulk nanocomposites and microcellular foams.

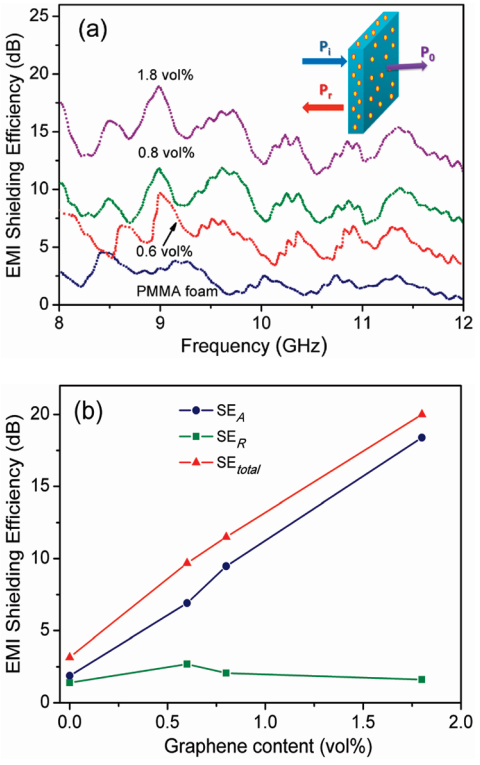

Figure 3. (a) EMI shielding efficiency of graphene−PMMA nanocomposite microcellular foams with different contents of graphene sheets. (b) The comparison of SE_{total}, microwave absorption (SE_A), and microwave reflection (SE_R) at 9 GHz.

Interestingly, the insulator-to-semiconductor transition of the foams shifts to lower graphene content compared to that of the bulk nanocomposites. The nanocomposite foam with ~0.6 vol % graphene sheets has an electrical conductivity of 3.80×10^{-5} S/m, which satisfies the antistatic criterion of 1×10^{-6} S/m.[4] With 0.8 vol % of graphene sheets, the conductivity of the PMMA foam approaches to 0.39 S/m. A much higher conductivity of 3.11 S/m was obtained in the microcelluar foam with only 1.8 vol % of graphene sheets, which is higher than the target conductivity value required for EMI shielding application.[13]

The EMI SE of the graphene−PMMA microcellular foams was determined in the microwave frequency range of 8−12 GHz (Figure 3). It is known that EMI SE is the sum of the reflection

from the material surface (SE_R), the absorption of electromagnetic energy (SE_A), and the multiple internal reflections (SE_M) of electromagnetic radiation. The reflection is related to the impedance mismatch between air and absorber; the absorption can be regarded as the energy dissipation of the electromagnetic microwave in the absorber; and the multiple reflections are considered as the scattering effect of the inhomogeneity within the materials. The inset of Figure 3 shows the mechanism involved in the EMI shielding process. The incident power (P_i) is divided into reflected power (P_r), the absorbed power, and the remaining power (P_0) at the output of the shielding.[29] From the measured scattering parameters, the power coefficients of reflectivity (R), transmissivity (T), and absorptivity (A) can be calculated, and their relationship is described as $R + T + A = 1$. The EMI SE of a material can be expressed as[10,30]

$$SE_{total} = 10\log(P_i/P_0) = SE_R + SE_A + SE_M \quad (1)$$

An attenuation of the incident EM radiation by a factor of 100 (i.e., 1% transmission) is equivalent to 20 dB of attenuation. SE_M can be negligible when SE ≥ 15 dB. The effective absorbance (A_{eff}) can be described as[9,10]

$$A_{eff} = (1 - R - T)/(1 - R) \quad (2)$$

With respect to the power of the effective incident electromagnetic wave inside the shielding material, the reflectance and effective absorbance can be conveniently expressed as[30,31]

$$SE_R = -10\log(1 - R) \quad (3)$$

and

$$SE_A = -10\log(1 - A_{eff}) = -10\log[T/(1 - R)] \quad (4)$$

The EMI SE curves of the graphene−PMMA microcellular foams with different contents of graphene sheets are shown in Figure 3a. Neat PMMA foam is obviously transparent to electromagnetic waves and exhibits hardly any EMI shielding efficiency. In contrast, with the increase of the graphene content, the EMI SE of the graphene−PMMA foams increases greatly, which is similar to the relationship between electrical conductivity and filler content and is consistent with the EMI shielding theory.[9] SE_{total} of the microcellular foam with 0.6 vol% graphene sheets is only slightly higher than that of neat PMMA foam. However, when the graphene content is just increased to 0.8 vol %, the SE_{total} value is above 7.5 dB in almost the entire frequency range measured in the experiment and approaches to 12 dB at the frequencies around 9.0 and 9.6 GHz. Furthermore, the microcellular foam with only 1.8 vol % graphene sheets exhibits high EMI SE of 13−19 dB at the frequencies from 8 to 12 GHz. As proposed by Gupta et al.,[18] the specific EMI shielding efficiency (EMI shielding efficiency divided by density) would be more appropriate when the shielding performance of polymer foams is compared to that of typical metals for aircraft and spacecraft applications. Thus, the specific EMI shielding efficiency of the PMMA foam with 1.8 vol % graphene was calculated to be 17−25 dB cm^3/g in the frequency range. Clearly, the dominant contribution to the EMI shielding properties of the graphene−PMMA foams results from the formation of an interconnected graphene network throughout the insulating PMMA matrix.[8,9,18]

Figure 3b shows plots of SE_{total}, SE_R, and SE_A of the graphene−PMMA nanocomposite foams as a function of graphene content at the frequency of 9 GHz. Obviously, the increase of graphene content leads to the improvement of both SE_{total} and SE_A and the contribution of microwave reflection is negligible over all the graphene contents. For the nanocomposite foam with

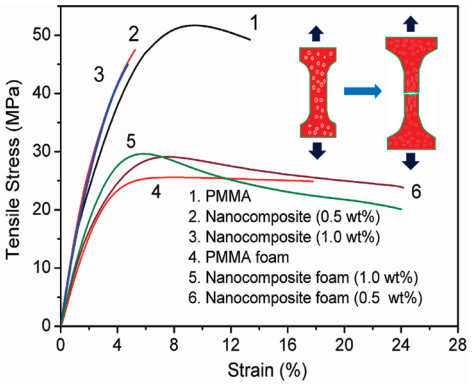

Figure 4. Stress−strain curves of PMMA and its graphene nanocomposites before and after foaming.

1.8 vol % graphene sheets, the values of SE_{total}, SE_A, and SE_R are 19, 18, and 1 dB, respectively. Therefore, the EMI shielding effect resulted from the absorption of the incident signal power entering the composite and its conductive dissipation through the nanocomposite foam thickness, confirming that microwave absorption is the dominant contribution to the total EMI SE of the graphene−PMMA microcellular foams.

It is noted that the EMI shielding performance of the microcellular foam with 1.8 vol% (5.0 wt %) graphene sheets is superior to that of polystyrene foam with 10 wt % CNFs, and is only slightly lower than that of polystyrene foam containing 7 wt % CNTs. Furthermore, almost all the electromagnetic waves were absorbed and attenuated by conductive dissipation in our graphene−PMMA foams, whereas reflection is the major contribution to EMI shielding for the CNF- and CNT-filled polystyrene foams. As EMI SE generally increases with increasing the specimen thickness,[31,32] it is reasonable to expect that the EMI SE value for the PMMA foam can be improved by increasing the specimen thickness and the graphene content. Even with the low loading of graphene sheets (1.8 vol %) and thin specimen (2.4 mm), the graphene−PMMA nanocomposite foam still exhibits a good EMI shielding effect, just slightly lower than the reported value (21 dB) for epoxy bulk nanocomposite with 15 wt % graphene sheets, and close to the target value of EMI SE required for practical application (~20 dB). These results indicate that graphene−PMMA nanocomposite microcellular foam can be used as an effective and lightweight EMI shielding material.

Different from the absorption dominant mechanism in our graphene−PMMA foams, Gupta et al. demonstrated that the primary EMI shielding mechanism of the polystyrene foams filled with CNFs and CNTs was reflection.[18,19] Similarly, CNT−filled epoxy and polyurethane nanocomposites also showed a reflection-dominant mechanism.[10,33] Recently, the EMI shielding properties of the graphene−epoxy nanocomposites was reported, but no shielding mechanism was discussed.[34]

Besides reflection and absorption, multiple reflection is another shielding mechanism, which refers to the reflection at various surfaces or interfaces in the shield.[11] This mechanism requires the presence of a large surface area or interface area in the shield. The microcellular structures of our graphene−PMMA foams provided a large cell−PMMA surface area, meanwhile the large specific surface area of graphene and its uniform dispersion in the matrix formed abundant graphene/PMMA interfacial area. Therefore, it is reasonable that the unique construction formed

Table 2. Specific Mechanical Properties of Bulk and Foamed PMMA and PMMA−Graphene Nanocomposites

samples	specific modulus (MPa/(kg/m^3))	elongation at break (%)	specific tensile toughness ($\times 10^2$) (MPa/(kg/m^3))	specific strength ($\times 10^3$) (MPa/(kg/m^3))
neat PMMA	1.32 ± 0.06	13 ± 2	0.46 ± 0.05	48.4 ± 0.3
composite (0.5 wt %)	1.48 ± 0.13	5 ± 1	0.13 ± 0.02	45.5 ± 0.3
composite (1.0 wt %)	1.56 ± 0.08	5 ± 2	0.11 ± 0.07	45.0 ± 0.4
neat PMMA foam	0.80 ± 0.04	18 ± 1	0.48 ± 0.01	25.2 ± 0.5
composite foam (0.5 wt %)	0.91 ± 0.04	24 ± 2	0.58 ± 0.06	27.3 ± 2.3
composite foam (1.0 wt %)	0. 96 ± 0.14	25 ± 2	0.47 ± 0.08	28.4 ± 2.6

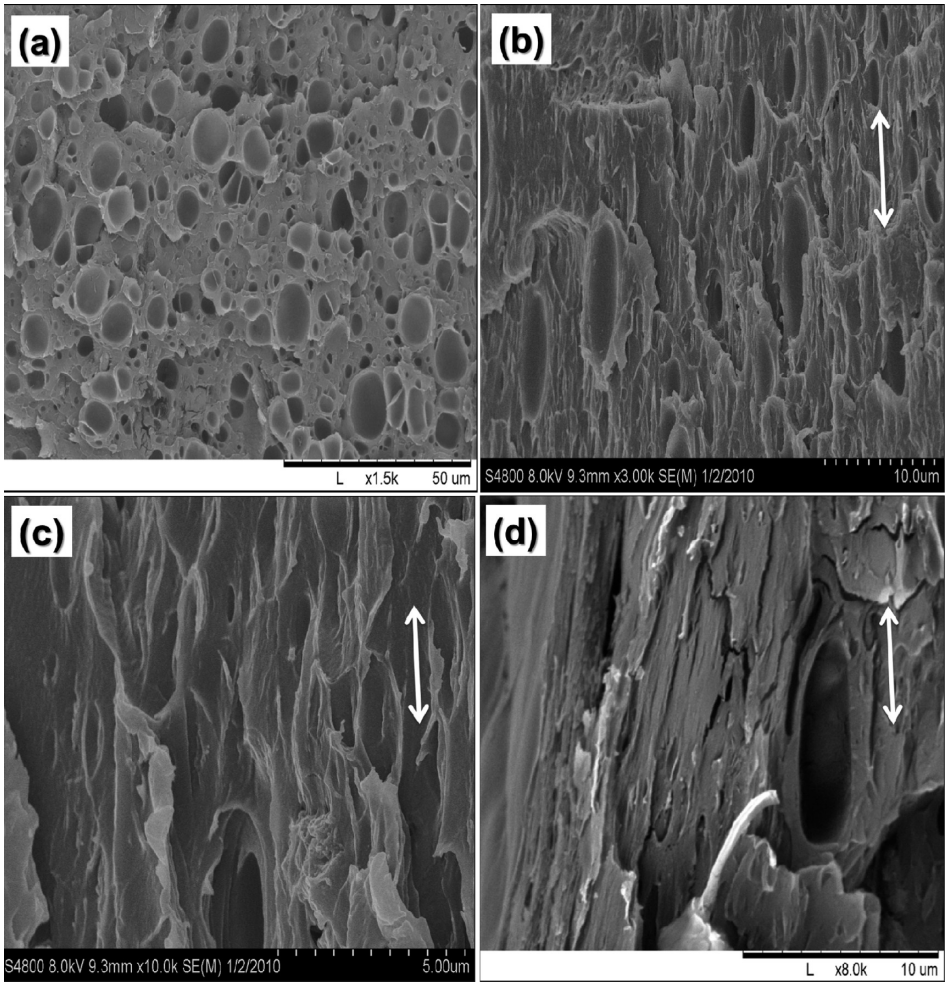

Figure 5. SEM images of PMMA/0.5 wt % graphene nanocomposite microcellular foam: (a) before stretching; (b) highly entangled microcellular cells near the fracture surface; (c, d) plastically stretched void network. Tensile direction is shown with double-headed arrows. Images b, c, and d were taken along a plane parallel to the tensile direction.

by graphene sheets in the graphene−PMMA foam favors microwave absorption. Incident microwaves entering the graphene−PMMA microcellular foam were reflected and scattered many times between cell−matrix interfaces and the graphene sheets, and were difficult to escape from the material until they were absorbed, similar to the case in ordered mesoporous carbon/fused silica composites.[30] Thus, the contribution of absorption to the total EMI SE of the graphene−PMMA foam is much higher than that of the reflection. These results indicate that the graphene−PMMA microcellular foams with excellent EMI SE would be suitable for the use as EMI shielding or electromagnetic absorption materials in the microwave frequency range.

The presence of microcellular cells made the brittle graphene−PMMA nanocomposite tough. Specific mechanical property (property divided by foam density) was used to normalize the effect of cells. The tensile toughness (the energy to fracture per unit volume) was calculated by integrating the area under the stress−strain curve.[35] Figure 4 shows the stress−strain curves of neat PMMA and its graphene nanocomposites before and after foaming. The addition of graphene sheets made neat PMMA even brittle, evidenced by the reduced ductility and tensile toughness. However, the ductility of the graphene−PMMA nanocomposites was significantly increased after foaming. As shown in Table 2, the PMMA foam with 0.5 wt % graphene sheets gives a fracture strain of 24% compared to 5% for its

bulk counterpart, leading to a 346% increment in tensile toughness from 13 to 58 MPa/(kg/m^3). For the foam containing 1.0 wt % graphene sheets, the tensile toughness is increased by more than 3 times.

The small cells of the graphene−PMMA microcellular foams are resistant to rupture and favorable for the improvement of toughness. The inset of Figure 4 presents a schematic of deformation of the microcellular foam under tensile loading. The uniform microcellular cells acted in a similar way as the cavitated rubber particles in rubber-toughened plastics.[36] Before tensile stretching, the microcellular cells showed nearly spherical morphology (Figure 5a). When the foam was subjected to an extension over the tensile yield stress, necking was observed with severe plastic growth of the microcellular cells near the fracture surface (Figure 5b). The material between voids was plastically stretched and transformed into fibrils (Figure 5c, d). With the highly stretching, the local stress intensification within the craze eventually enlarged the void content by coalescence of voids. This toughness mechanism of microcellular cells was also observed in PS and PC foams[35,37] and polypropylene nanocomposites with submicrometer voids.[38] In addition, the incorporation of graphene sheets reinforced PMMA foam. With 1.0 wt % graphene sheets, the specific modulus of the PMMA foam increased by 18% and its specific yield strength increased by 13% (Table 2). These improvements were attributed to the reinforcement of cell walls/junctions by the graphene.

CONCLUSION

Graphene−PMMA nanocomposites were prepared by blending and then foamed by using an environmentally benign subcritical CO_2 foaming technique. The novel graphene−PMMA nanocomposite microcellular foams are electrically conductive and their insulator-to-semiconductor transition shifts to lower graphene content compared to that of the bulk nanocomposites. The graphene−PMMA foam with a low graphene loading of 1.8 vol % exhibits not only a high conductivity of 3.11 S/m, but also a good EMI shielding efficiency of 13−19 dB at the frequencies from 8 to 12 GHz. The EMI shielding efficiency is mainly attributed to the absorption rather than the reflection in the investigated frequency range. Interestingly, the presence of microcellular cells greatly improves the ductility and tensile toughness of the brittle graphene−PMMA nanocomposites. This work provides a promising methodology to fabricate tough and lightweight graphene−PMMA nanocomposite microcellular foams with superior electrical and EMI shielding properties.

ASSOCIATED CONTENT

Supporting Information. Preparation information and additional figure (PDF). This material is available free of charge via the Internet at http://pubs.acs.org.

AUTHOR INFORMATION

Corresponding Author

*Fax: +86-10-6442 8582 (Z.-Z.Y.); +86-574-8668 5186 (W.-G. Z.). E-mail: yuzz@mail.buct.edu.cn (Z.-Z.Y.); wgzheng@nimte.ac.cn (W.-G.Z.).

REFERENCES

(1) Kuilla, T.; Bhadra, S.; Yao, D.; Kim, N. H.; Bose, S.; Lee, J. H. *Prog. Polym. Sci.* **2010**, *35*, 1350–1375.
(2) Loh, K. P.; Bao, Q. L.; Ang, P. K.; Yang, J. X. *J. Mater. Chem.* **2010**, *20*, 2277–2289.
(3) Geim, A. K. *Science* **2009**, *324*, 1530–1534.
(4) Stankovich, S.; Dikin, D. A.; Dommett, G. H. B.; Kohlhaas, K. M.; Zimney, E. J.; Stach, E. A.; Piner, R. D.; Nguyen, S. T.; Ruoff, R. S. *Nature* **2006**, *442*, 282–286.
(5) Geim, A. K.; Novoselov, K. S. *Nat. Mater.* **2007**, *6*, 183–191.
(6) He, H. K.; Gao, C. *Chem. Mater.* **2010**, *22*, 5054–5064.
(7) He, H. K.; Gao, C. *ACS Appl. Mater. Interfaces* **2010**, *2*, 3201–3210.
(8) Fugetsu, B.; Sano, E.; Sunada, M.; Sambongi, Y.; Shibuya, T.; Wang, X.; Hiraki, T. *Carbon* **2008**, *46*, 1256–1258.
(9) Kim, H. M.; Kim, K.; Lee, C. Y.; Joo, J.; Cho, S. J.; Yoon, H. S.; Pejaković, D. A.; Yoo, J. W.; Epstein, A. J. *Appl. Phys. Lett.* **2004**, *84*, 589–591.
(10) Li, N.; Huang, Y.; Du, F.; He, X. B.; Lin, X.; Gao, H. J.; Ma, Y. F.; Li, F. F.; Chen, Y. S.; Eklund, P. C. *Nano Lett.* **2006**, *6*, 1141–1145.
(11) Al-Saleh, M. H.; Sundararaj, U. *Carbon* **2009**, *47*, 1738–1746.
(12) Liang, J. J.; Huang, Y.; Zhang, L.; Wang, Y.; Ma, Y. F.; Guo, T. Y.; Chen, Y. S. *Adv. Funct. Mater.* **2009**, *19*, 2297–2302.
(13) Thomassin, J. M.; Pagnoulle, C.; Bednarz, L.; Huynen, I.; Jerome, R.; Detrembleur, C. *J. Mater. Chem.* **2008**, *18*, 792–796.
(14) Park, S. H.; Theilmann, P.; Yang, K. Q.; Rao, A. M.; Bandaru, P. R. *Appl. Phys. Lett.* **2010**, *96*, 043115.
(15) Zhang, H. B.; Zheng, W. G.; Yan, Q.; Yang, Y.; Lu, Z. H.; Wang, J. W.; Ji, G. Y.; Yu, Z. Z. *Polymer* **2010**, *51*, 1191–1196.
(16) Xie, S. H.; Liu, Y. Y.; Li, J. Y. *Appl. Phys. Lett.* **2008**, *92*, 243121.
(17) Xu, X. B.; Li, Z. M.; Shi, L.; Bian, X. C.; Xiang, Z. D. *Small* **2007**, *3*, 408–411.
(18) Yang, Y. L.; Gupta, M. C. *Nano Lett.* **2005**, *5*, 2131–2134.
(19) Yang, Y. L.; Gupta, M. C.; Dudley, K. L.; Lawrence, R. W. *Adv. Mater.* **2005**, *17*, 1999–2003.
(20) Esawi, A. M. K.; Farag, M. M. *Mater. Design* **2007**, *28*, 2394–2401.
(21) Li, D.; Muller, M. B.; Gilje, S.; Kaner, R. B.; Wallace, G. G. *Nat. Nanotechnol.* **2008**, *3*, 101–105.
(22) Lee, L. J.; Zeng, C. C.; Cao, X.; Han, X. M.; Shen, J.; Xu, G. J. *Compos. Sci. Technol.* **2005**, *65*, 2344–2363.
(23) Zeng, C. C.; Han, X. M.; Lee, L. J.; Koelling, K. W.; Tomasko, D. L. *Adv. Mater.* **2003**, *15*, 1743–1743.
(24) Verdejo, R.; Barroso-Bujans, F.; Rodriguez-Perez, M. A.; de Saja, J. A.; Lopez-Manchado, M. A. *J. Mater. Chem.* **2008**, *18*, 2221–2226.
(25) Rafiee, M. A.; Rafiee, J.; Srivastava, I.; Wang, Z.; Song, H.; Yu, Z.-Z.; Koratkar, N. *Small* **2010**, *6*, 179–183.
(26) Zhao, X.; Zhang, Q. H.; Chen, D. J.; Lu, P. *Macromolecules* **2010**, *43*, 2357–2363.
(27) Zhang, H.-B.; Wang, J.-W.; Yan, Q.; Zheng, W.-G.; Chen, C.; Yu, Z.-Z. *J. Mater. Chem.* **2011**, DOI:10.1039/C1JMI0099H.
(28) Yavari, F.; Rafiee, M. A.; Rafiee, J.; Yu, Z. Z.; Koratkar, N. *ACS Appl. Mater. Interfaces* **2010**, *2*, 2738–2743.
(29) Thomassin, J. M.; Lou, X.; Pagnoulle, C.; Saib, A.; Bednarz, L.; Huynen, I.; Jerome, R.; Detrembleur, C. *J. Phys. Chem. C* **2007**, *111*, 11186–11192.
(30) Wang, J. C.; Xiang, C. S.; Liu, Q.; Pan, Y. B.; Guo, J. K. *Adv. Funct. Mater.* **2008**, *18*, 2995–3002.
(31) Li, B.-W.; Shen, Y.; Yue, Z.-X.; Nan, C.-W. *Appl. Phys. Lett.* **2006**, *89*, 132504.
(32) Das, N. C.; Liu, Y.; Yang, K.; Peng, W.; Maiti, S.; Wang, H. *Polym. Eng. Sci.* **2009**, *49*, 1627–1634.
(33) Liu, Z. F.; Bai, G.; Huang, Y.; Ma, Y. F.; Du, F.; Li, F. F.; Guo, T. Y.; Chen, Y. S. *Carbon* **2007**, *45*, 821–827.
(34) Liang, J. J.; Wang, Y.; Huang, Y.; Ma, Y. F.; Liu, Z. F.; Cai, F. M.; Zhang, C. D.; Gao, H. J.; Chen, Y. S. *Carbon* **2009**, *47*, 922–925.
(35) Collias, D. I.; Baird, D. G. *Polym. Eng. Sci.* **1995**, *35*, 1167–1177.

(36) Dasari, A.; Yu, Z. Z.; Mai, Y. W. *Polymer* **2009**, *50*, 4112–4121.
(37) Collias, D. I.; Baird, D. G.; Borggreve, R. J. M. *Polymer* **1994**, *35*, 3978–3983.
(38) Dasari, A.; Zhang, Q.-X.; Yu, Z.-Z.; Mai, Y.-W. *Macromolecules* **2010**, *43*, 5734–5739.